

Coupling to the continuous spectrum and HFB approximation

K. Bennaceur,^aJ.F. Berger^b, B. Ducomet^b

^a*IPN Lyon, CNRS IN2P2 Université Claude Bernard Lyon I,
43 Bd du 11 Novembre 1918,
69622 Villeurbanne Cedex, France*

^b*CEA-Département de Physique Théorique et Appliquée,
BP 12, 91680 Bruyères-le-Chatel, France*

Abstract

We propose a new method to solve the Hartree-Fock-Bogoliubov equations for weakly bound nuclei whose purpose is to improve the treatment of the continuum when a finite range two-body interaction is used. We replace the traditional expansion on a discrete harmonic oscillator basis by a mixed eigenfunction expansion associated with a potential that explicitly includes a continuous spectrum. We overcome the problem of continuous spectrum discretization by using a resonance expansion.

Key words: Hartree-Fock calculation, Unstable nuclei, Finite-range interaction
PACS: 21.60.Jz, 02.70.-c, 21.30.Fe

1 Introduction

In many problems of present-day nuclear physics (structure of the ground state of nuclei close to drip lines, description of weakly bound or unbound excited states, decay of isomeric states), one has to explicitly take into account the continuum of scattering states in addition to the discrete spectrum of bound states. A convenient approach to these problems is provided by the mean-field theory in which pairing correlations are included in a self-consistent way through the Hartree-Fock-Bogoliubov (HFB) formalism [1,2]. In this method a set of quasi-particle excitations together with their vacuum is obtained, which forms the basis for a description of ground state properties and spectra. In

Email address: k.bennaceur@ipnl.in2p3.fr (K. Bennaceur,).

principle, quasi-particle states, when expressed in terms of the single-particle eigenstates of a one-body hamiltonian, are always superpositions of states belonging to both the discrete and continuous spectra [3,4]. In ordinary stable nuclei, the continuum part of quasi-particle states is usually neglected, as ground state properties and low-energy excitations mainly depend on the discrete quasi-particle states representing occupied and negative energy unoccupied single-particle orbitals. So, quasi-particles are often obtained using expansions on a discrete basis of orthonormal square-integrable functions.

A very different situation is encountered in weakly bound nuclei, where the gap between the last occupied single-particle level and the continuum of positive energy states may become smaller than a few MeV. In this case, the residual pairing interaction is able to induce a significant coupling between the discrete and continuum single-particle states and the contribution of the continuum to quasi-particle states cannot be neglected.

In such a situation, new numerical methods for solving the HFB equations have to be implemented, which more or less implicitly, amount to introduce a suitable discretization of the continuum. With these methods, not only the contribution of the continuum to quasi-particle states can be obtained, but also a description of quasi-particles belonging to the continuous spectrum, including resonances. Let us note that such a treatment is necessary to reproduce the unusual properties of weakly bound nuclei such as halos and neutron skins.

Several techniques have been proposed in the past along these lines: lattice calculations [5], Basis-Spline Galerkin lattice [6], methods using the local-scale point transformation of the spherical harmonic oscillator wave functions [7], which are adapted to calculations involving zero-range two-body interactions such as the Skyrme forces. Another approach, based on the Kamimura-Gauss basis [8] has been reported recently [9]. It appears to be a promising technique for both zero range and finite range forces. Recently, a method has been proposed where the HFB equations are solved in a spherical box with exact boundary conditions for scattering states [10,11]. In these methods, the HFB equations are usually expressed in space coordinates, which is especially convenient when a zero-range nucleon-nucleon interaction is used, and interesting results have been obtained in this context [3,12,13].

In the case of the finite range Gogny interaction [2], the HFB equations have always been solved by expanding the quasi-particle states on a finite discrete basis of orthonormal functions. In view of computational convenience, the latter are usually chosen as the eigenfunctions of an harmonic oscillator (HO), whose geometry and symmetries are adapted to the nuclear states to be studied. The HFB equations are then expressed in matrix form, and they are solved by using an iterative procedure. Namely, at iteration n , the set of individual

wave functions $\{\psi_i^{(n)}\}$ is expanded on a finite basis of generalized eigenstates of a reference hamiltonian $H^{(n)}$, generally taken as $T + V_{HO}^{(n)}$, where $V_{HO}^{(n)}$ is an harmonic oscillator potential:

$$\psi_i^{(n)} = \sum_{p=1}^{N_{max}} C_{i,p}^{(n)} \varphi_p^{(n)}. \quad (1)$$

The $\varphi_p^{(n)}$ are explicitly known and the unknown coefficients $C_{i,p}^{(n)}$ are determined using matrix diagonalization techniques.

This simple choice has been found to be appropriate for computing the properties of well bound nuclei, the convergence of the iterative procedure being obtained with a reasonable number of iterations [2,14]. In practice, the sum in (1) is truncated to a number of states N_{max} corresponding to a number of HO shells ranging from 6-8 in light nuclei up to 16-20 in heavy and superheavy nuclei.

On the other hand, in exotic nuclei close to drip-lines, weakly bound single-particle states acquire a spatial extension so large that the use of expansions on HO wave functions such as (1) requires prohibitively large values of N_{max} . In this case, as mentioned above, an alternative method of solving the HFB equations has to be found.

A natural way to avoid this difficulty is to change the reference potential from which the basis is built. Let us recall the well-known “decomposition of unity” on a complete basis of generalized eigenstates, associated with a reference hamiltonian, a sum of kinetic and potential terms $H = T + V$. We assume that V is short-ranged and negative for small r . This decomposition formula can be written formally as

$$\mathbf{1} = \sum_{n=1}^N |\varphi_n\rangle\langle\varphi_n| + \int |\varphi(\cdot, k)\rangle\langle\varphi(\cdot, k)| dk, \quad (2)$$

where the first (resp. second) contribution corresponds to the discrete (resp. continuous) spectrum of H .

Numerical simulations [15,16] show that the continuous contribution in (2) can be neglected in the expansion of single particle states provided the gap between the energy of the last occupied state $|E_N|$ and the continuous threshold is large enough, which is the case in stable nuclei.

As mentioned before, for nuclei near instability, the gap is small and the continuous contribution in (2) has to be taken into account.

A new difficulty then appears: a numerical treatment based on equation (2)

requires to introduce both a discretization and a cut-off in the integral involving continuous states. This leads to a finite expansion upon discrete basis states which is not necessarily less expensive than the one in (1), unless one can identify a few states carrying a predominant contribution of the continuous part in (2). As shown in a simplified model [17], such a discretization would probably lead to the same numerical difficulties as above, as the necessary truncation of the integral in (2) is not likely to be less expensive than a sum with large N_{max} in (1).

As a matter of fact one knows that the so-called metastable or resonant states corresponding to complex singularities of the resolvent give important contributions to the density of states. These states decay exponentially in time, preventing them to be considered as part of the spectrum, although they correspond to long-living nuclear configurations. Moreover it has been soon recognized (see [18] and references therein) that, despite their pathological asymptotic behaviour, these unstable states could be used as generalized eigenfunctions that can be used to describe resonance phenomena in nuclear collisions. In this framework, a given state is expanded on a set of functions that includes resonant functions on the same footing as bound state eigenfunctions.

The drawbacks of such a procedure are well known: as the resulting problem loses its self-adjointness, the complex spectrum has to be reinterpreted together with the associated wave functions. However such expansions have been frequently used to describe various physical situations (potential and obstacle scattering, nuclear reactions... [19]). Recently, this approach has also been used to treat the problem of multiconfiguration mixing within the nuclear shell model [20].

Our purpose is to show that this old idea may be applied in a simple way to self-consistent computations when loosely bound or metastable states are expected, which is precisely the case in HFB computations for heavy nuclei, especially those which are close to drip-lines.

This paper is organized as follows. In Sec. 2, we consider a model where the Schrödinger equation is solved in a bounded domain, and we apply it to a simplified one-body problem. In Sec. 3 some numerical experiments are presented, while Sec. 4 briefly presents our conclusions.

2 The problem in a bounded domain

Classically, in order to derive generalized eigenfunction expansions such as (2), one first computes the Green function associated to the problem and one uses complex analysis to continue this Green function and study its singularities.

Then, by applying the Cauchy residue theorem, one obtains (2), where the sum corresponds to the discrete spectrum, and the integral takes into account the continuous part of the spectrum (see Appendix A).

A natural way to avoid the delicate discretization of the continuous contribution in (2) is to restrict the initial problem to a bounded region Ω , where one expects that most of the physics takes place, and to impose “transparent” boundary conditions reflecting the properties of the exterior (unbounded) domain. In fact, this last point deserves a special comment. It is clear that the kind of artificial conditions we impose on the boundary must be of particular nature in order to mimic the behaviour of the “exterior world”, in a transparent way: the waves produced in the interior region must not be disturbed (reflected) by the boundary. For example, a standard Dirichlet or Von Neumann boundary conditions would lead to a problem essentially different from the one we want to solve and would produce results without clear connection with the solution of our original problem. One can check easily in particular that Dirichlet condition would lead to nothing but a Fourier series expansion, which makes the obtained solution strongly domain-dependent.

One can show that this kind of “transparent” boundary conditions, which has been developed in the acoustic domain and more recently in the Schrödinger context (see [21] and references therein) leads to a complex condition producing a non-selfadjoint problem: this is the price to pay for “replacing the exterior by the boundary”.

By restricting the domain, one can hope to get improved asymptotic properties for the modified Green functions, allowing one to bypass the integral along the physical cuts in (2). As a consequence, complex isolated singularities appear outside the imaginary axis, coming from the artificial complex conditions at the boundary of Ω .

To our knowledge, this idea goes back to Kapur and Peierls [22] who first introduced in the thirties non self-adjoint flux conditions associated to Schrödinger equations, a method which has been widely used in the context of nuclear reactions [18].

2.1 *The model*

In the particular situation of the square well potential, the above method can be worked out in a very simple way. The idea is to replace the harmonic oscillator by a new reference potential V such that the hamiltonian $H = T + V$ has a continuous spectrum, in order to describe more accurately the loosely bound states and, if necessary, metastable states.

As we expect that the physics takes place in the region Ω where the potential is non-zero, we restrict the dynamics to Ω and we impose a boundary condition at the boundary which mimics the external scattering behaviour.

To be specific, let us consider the Schrödinger equation for a particle in a compactly supported spherically symmetric potential V :

$$\left(-\frac{d^2}{dr^2} + V(r)\right) \varphi_k(r) = k^2 \varphi_k(r), \quad \text{for } r \in \Omega = (0, r_0). \quad (3)$$

Where we have considered $\hbar^2/2m = 1$ and an orbital momentum $\ell = 0$. As a new reference potential V , we take the square well defined as:

$$V(r) = \begin{cases} -V_0, & \text{for } r < r_0, \\ 0, & \text{otherwise,} \end{cases} \quad (4)$$

where $V_0 > 0$ and $r_0 > 0$.

We chose the square well because the associated eigenfunctions are rather elementary (Bessel functions). Moreover, in order to simplify the arguments we restrict the analysis to s -waves, in which case the eigenfunctions are simply sine and cosine functions.

As an extra boundary condition for $r = r_0$, we choose the free radiation condition:

$$\left(\frac{d}{dr} - ik\right) \varphi_k(r) = 0, \quad \text{for } r = r_0. \quad (5)$$

From the above discussion about “transparent” boundary conditions, we stress that the non-selfadjoint boundary condition (5) amounts to fix an imaginary flux condition reflecting exactly the physical radiation behaviour at infinity for the free Schrödinger equation. We feel that this choice corresponds to our purpose to produce the smallest perturbation near the artificial boundary $r = r_0$.

The problem (3)-(5) is easily solved by computing the corresponding Green function (see Appendix A), giving simple explicit expressions for the associated eigenfunctions and the following expansion for any function $f \in L^2(0, r_0)$:

$$f(r') = \sum_n \frac{k_n}{i + k_n r_0} \left(\int_0^{r_0} \sin p_n r f(r) dr \right) \sin p_n r', \quad (6)$$

where the k_n are the solutions both, real and complex, of the equation :

$$p_n \cot p_n r_0 = ik_n, \quad (7)$$

with $p_n = (k_n^2 + V_0)^{1/2}$. For real roots we recover bound and virtual state eigenfunctions, while for non real ones we get resonant and anti-resonant eigenfunctions.

2.2 Application to HFB problems

Let us consider the familiar Hartree-Fock-Bogoliubov equations:

$$\begin{pmatrix} T + \mathcal{U} & \mathcal{V} \\ \mathcal{V} & -T - \mathcal{U} \end{pmatrix} \begin{pmatrix} \psi_1 \\ \psi_2 \end{pmatrix} = \begin{pmatrix} E + \lambda & 0 \\ 0 & E - \lambda \end{pmatrix} \begin{pmatrix} \psi_1 \\ \psi_2 \end{pmatrix}, \quad (8)$$

where the particle-hole and particle-particle potentials \mathcal{U} and \mathcal{V} depend on ψ_1 and ψ_2 .

In order to solve this non linear eigenvalue problem we expand the unknown wave functions ψ_1 and ψ_2 on our reference basis, suitably truncated up to a rank N , depending on the desired accuracy:

$$\psi_1 = \sum_{n=0}^N a_n \varphi_n, \text{ and } \psi_2 = \sum_{n=0}^N b_n \varphi_n, \quad (9)$$

where

$$\varphi_n(r) = \sin p_n r \quad (10)$$

and the coefficients p_n are obtained by solving the transcendental equation (7).

Replacing the functions $\psi_1(r)$ and $\psi_2(r)$ by there expansions, multiplying on the left by $\varphi_m^*(r)$ and integrating, one gets the following expressions for (8):

$$\begin{cases} \sum_{n=0}^N (\mathbf{T}_{mn} + \mathbf{U}_{mn}) a_n + \mathbf{V}_{mn} b_n = (E + \lambda) \sum_{n=0}^N \mathbf{R}_{mn} a_n, \\ \sum_{n=0}^N \mathbf{V}_{mn} a_n - (\mathbf{T}_{mn} + \mathbf{U}_{mn}) b_n = (E - \lambda) \sum_{n=0}^N \mathbf{R}_{mn} b_n. \end{cases} \quad (11)$$

or in matrix form:

$$\begin{pmatrix} \mathbf{T} + \mathbf{U} & \mathbf{V} \\ \mathbf{V} & -\mathbf{T} - \mathbf{U} \end{pmatrix} \Psi = \begin{pmatrix} (E + \lambda) \mathbf{R} & 0 \\ 0 & (E - \lambda) \mathbf{R} \end{pmatrix} \Psi \quad (12)$$

where \mathbf{T} , \mathbf{U} , \mathbf{V} and \mathbf{R} are complex hermitian matrices and Ψ is the column vector of components $c_i \equiv (a_1, \dots, a_N, b_1, \dots, b_N)$.

The equation (12) is a generalized eigenvalue problem, from which the coefficients of the expansion (10) together with the eigenvalues E can be obtained.

If we solve the problem using only the functions φ_n (corresponding to $\ell = 0$), these elements are rather simple and in many cases they can be computed analytically.

Some care must be taken in the evaluation of the kinetic energy \mathbf{T} . As discussed before, the expansion we use is valid only for $r \in (0, r_0)$ and expansion (9) concerns only the part of the functions $\psi_{1,2}(r)$ defined in this interval. Consequently equations (9) have to be replaced by:

$$Y(r_0 - r)\psi_1(r) = \sum_n a_n \varphi_n(r), \text{ and } Y(r_0 - r)\psi_2(r) = \sum_n b_n \varphi_n(r), \quad (13)$$

where $Y(r_0 - r)$ is the Heaviside function. Taking the second derivative of this function, one gets:

$$\frac{d^2}{dr^2} \left[Y(r_0 - r)\psi_i(r) \right] = Y(r_0 - r) \frac{d^2\psi_i(r)}{dr^2} - \delta(r_0 - r) \left. \frac{d\psi_i(r)}{dr} \right|_{r=r_0} \quad (14)$$

As a consequence, the matrix elements of the kinetic energy T are:

$$\begin{aligned} \mathbf{T}_{mn} &= -\frac{\hbar^2}{2m} \int_0^{r_0} \varphi_m^*(r) \left[\Delta - \delta(r_0 - r) \frac{d}{dr} \right] \varphi_n(r) dr \\ &= \frac{\hbar^2 k_n^2}{2m} \mathbf{R}_{mn} + \frac{\hbar^2 k_n^2}{2m} \sin(k_m r_0) \cos(k_n r_0) \end{aligned} \quad (15)$$

They are computed in the same way as those of \mathbf{R} (see relation (11)). Let us note that similar formulas have to be employed if the potentials \mathcal{U} and \mathcal{V} contain velocity-dependent contributions for example in the spin-orbit components.

In the case of a nucleon-nucleon force of simple form (Skyrme or Gogny forces), the matrices \mathcal{U} and \mathcal{V} can be calculated analytically. Let us note that since \mathbf{T} and \mathbf{R} are hermitian matrices, the reality of the eigenvalues in equation (11) is insured. Finally the Coulomb potential can also be calculated analytically.

2.3 Canonical states

In order to interpret the HFB results, let us introduce the normal reduced density $\rho(r, r')$:

$$rr'\rho(r, r') = \sum_k \psi_2^{(k)}(r) \psi_2^{(k)*}(r'), \quad (16)$$

where $\psi_2^{(k)}$ denotes the lower component of the k^{th} solution of equation (12). With a similar notation, the abnormal reduced density $\tilde{\rho}(r, r')$ is given by:

$$rr'\tilde{\rho}(r, r') = - \sum_k \psi_2^{(k)}(r) \psi_1^{(k)*}(r'), \quad (17)$$

Using expansion (9), these relations become:

$$rr'\rho(r, r') = \sum_k \sum_{i,j} b_i^{(k)} b_j^{(k)*} \varphi_i(r) \varphi_j^*(r'), \quad (18)$$

and:

$$rr'\tilde{\rho}(r, r') = - \sum_k \sum_{i,j} b_i^{(k)} a_j^{(k)*} \varphi_i(r) \varphi_j^*(r'), \quad (19)$$

for $0 \leq r, r' \leq r_0$.

The interpretation of these quantities is clear (see for example [1]). The normal density is localized as soon as the chemical parameter λ is negative. The canonical basis $\{\bar{\psi}_i\}$ is defined as the set of eigenvectors of the normal density:

$$\int dr' rr' \rho(r, r') \bar{\psi}_i(r') = v_i^2 \bar{\psi}_i(r), \quad (20)$$

where the eigenvalues v_i^2 are the occupation probabilities of the corresponding canonical states. It is straightforward to show that if the $\bar{\psi}_i$ are expanded in the same way as the quasi-particle wave functions, this equation corresponds to:

$$\rho \mathbf{R} \bar{\Psi}_i = v_i^2 \bar{\Psi}_i, \quad (21)$$

where $\bar{\Psi}_i$ is the vector built with the coefficients of the expansion of $\bar{\psi}_i(r)$ and ρ is the matrix defined by:

$$\rho_{ij} = \sum_k b_i^{(k)} b_j^{(k)*}. \quad (22)$$

It is important to stress that ρ_{ij} is not properly speaking a representation of the normal density since the set of functions $\{\varphi_i\}$ does not form a basis.

Finally, we define the energies of the canonical states as the diagonal matrix element of the Hartree-Fock Hamiltonian in the basis of the canonical states [1]:

$$\epsilon_i = \langle \bar{\Psi}_i | H | \bar{\Psi}_i \rangle \quad (23)$$

This term can be easily written once the coefficients of the expansion of the canonical states are known.

3 Numerical simulations

To illustrate this method we have chosen to solve a simplified problem of HFB type with spherical symmetry. We consider the following equations:

$$\begin{pmatrix} T + \mathcal{U} & \mathcal{V} \\ \mathcal{V} & -T - \mathcal{U} \end{pmatrix} \begin{pmatrix} \psi_1 \\ \psi_2 \end{pmatrix} = \begin{pmatrix} E + \lambda & 0 \\ 0 & E - \lambda \end{pmatrix} \begin{pmatrix} \psi_1 \\ \psi_2 \end{pmatrix} \quad (24)$$

where T is the kinetic energy operator, \mathcal{U} and \mathcal{V} are respectively the particle-hole and particle-particle mean-fields. We do not take into account the possible effects of a Coulomb field or of a spin-orbit potential, although this would not lead to any difficulties in the treatment.

3.1 Hartree-Fock case (no pairing)

We first consider the case without pairing, *i.e.* $\mathcal{V} = 0$. In this case, the Lagrange multiplier λ is not needed any more and we can omit it in the equations. We want to check the ability of our method to construct the correct bound and resonant states associated with a given potential. To this aim, we consider the gaussian potential used in [23]:

$$\mathcal{U}(r) = 5e^{-0.25(r-3.5)^2} - 8e^{-0.2r^2} \quad (25)$$

This potential is given in MeV and the radial coordinate in fm in units where $\hbar^2/2m = 1/2$ MeV.fm². This potential has a rich spectrum in all partial waves and the discrete states have been calculated with high accuracy in [23]. The energies and widths of the discrete states up to 10 MeV are reported in table 1.

To build the set of functions (10) we have used a rectangular well of depth 30 MeV and radius 12 fm. By solving equation (7) we have found 30 bound states and 29 virtual states. We complete this set with the lowest resonances and companion anti-resonances. The corresponding functions are not orthogonal and we cannot build the matrix \mathbf{R} using all of them, otherwise the generalized eigenvalue problem (12) would be – at least numerically – singular. In order to reject some functions we use the following procedure: we build the full matrix \mathbf{R} , using all functions and try to invert it with a simple Gauss method.

ℓ	E	Γ
0	-4.571 183	0
0	-0.884 281	0
0	2.252 381	0.000 118
0	4.500 948	0.247 951
0	6.008 281	2.516 116
0	7.587 937	6.266 307
1	-2.619 884	0
1	0.807 635	~ 0
1	3.577 387	0.013 017
1	5.312 240	1.063 163
1	6.845 729	4.224 511
1	8.427 005	8.441 884

ℓ	E	Γ
2	-0.759 532	0
2	2.384 152	0.000 083
2	4.659 669	0.217 375
2	6.163 324	2.408 615
3	1.009 032	~ 0
3	3.810 922	0.008 196
3	5.581 406	0.932 281
3	7.091 723	4.003 469
4	2.676 525	0.000 028
4	5.025 176	0.148 085
4	6.522 260	2.137 256
4	8.059 380	5.759 133

Table 1

Discrete levels associated with the potential defined by (25). The energies and widths are determined by looking at the position of the poles of the S matrix in the complex energy plane.

During this calculation, if we encounter a pivot smaller than a given value, then we reject the corresponding function. As a result, most of the times, we cannot use simultaneously bound and virtual states, because those two sets span spaces which are almost identical. In this example, we have been led to keep the 30 bound states, 3 resonances and 3 anti-resonances. The total number of functions used to expand the solutions is then 36.

Because of the absence of pairing field, the matrix equation (12) is equivalent to the Hartree-Fock problem:

$$[\mathbf{T} + \mathbf{U}]\Psi = E\mathbf{R}\Psi \quad (26)$$

The matrix elements of the matrices \mathbf{T} , \mathbf{R} and \mathbf{U} can be computed analytically. Their expressions are given in Appendix B. After computing the matrices in (26) and diagonalizing the matrix $\mathbf{R}^{-1}(\mathbf{T}+\mathbf{U})$ we obtain a set of eigenvalues and eigenvectors that we normalize to 1 inside the domain $(0, r_0)$.

We have reported in table 2 the eigenvalues obtained below 10 MeV. We can see that the values from table 1 are nicely reproduced. The bound states are given with an accuracy of five to six significant digits for the $\ell = 0$ and $\ell = 2$

$\ell = 0$	$\ell = 1$	$\ell = 2$	$\ell = 3$	$\ell = 4$
-4.571 182	-2.605 981	-0.759 533	0.186 392	0.229 617
-0.884 280	0.130 394	0.153 058	0.535 440	0.585 189
0.118 909	0.471 894	0.497 537	1.009 141	1.120 116
0.458 980	0.836 844	1.023 303	1.065 186	1.800 000
0.980 599	0.995 157	1.692 437	1.738 986	2.592 748
1.644 922	1.660 949	2.384 031	2.524 324	2.676 568
2.252 302	2.436 584	2.472 184	3.387 049	3.466 495
2.418 722	3.283 319	3.327 296	3.811 796	4.374 556
3.265 180	3.617 422	4.193 201	4.290 813	4.993 930
4.106 893	4.170 489	4.675 124	5.120 114	5.392 091
4.546 091	4.968 645	5.215 890	5.742 917	6.207 120
5.140 059	5.605 141	6.024 047	6.469 599	7.002 387
5.946 712	6.379 345	6.841 667	7.342 215	7.878 341
6.773 633	7.256 568	7.743 484	8.286 709	8.849 874
7.684 636	8.230 319	8.731 860	9.300 691	9.897 122
8.679 769	9.252 138	9.793 386		
9.746 902				

Table 2

Eigenvalues obtained by diagonalizing the matrix equation (26). The boldface numbers correspond to the energies of the bound states and of the scattering states strongly localized inside the potential.

states. The narrow resonances are also very well reproduced. The discrepancies between the values in table 1 and 2 for the resonances energies are mainly due to their widths. The wide resonances found in table 1 by computing the S matrix cannot be seen directly in table 2 because they spread over a number of scattering states. The states with $\ell = 1$ are not so well reproduced, but we have checked that the agreement is better if we use more functions to expand the solutions (in this example, all the results are obtained by using 36 functions to expand the solutions). A plausible explanation concerning this deficiency is the following: the set of functions used to expand the solutions behaves like r in the limit $r \rightarrow 0$, so the convergence is supposed to be slower for partial waves with $\ell > 0$, the most important consequences are seen on waves with $\ell = 1$ because these functions have a significant amplitude near the origin where they are not supposed to be correctly reproduced. This effect is smoothed for higher partial waves because the centrifugal term prevent them to “explore” the vicinity of the origin. It is really remarkable to see that the

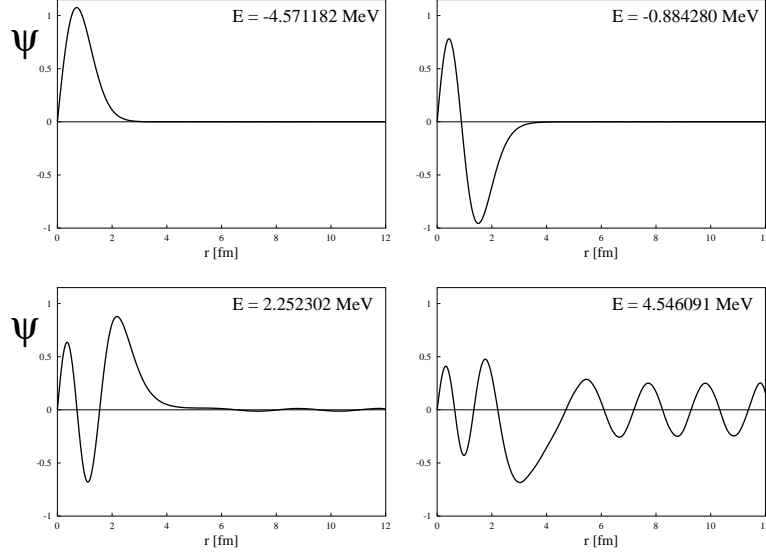


Fig. 1. Wave functions obtained for $\ell = 0$. Upper-left and Upper-right: the two bound states at -4.571182 MeV and -0.884280 MeV. Lower-left: the first resonance at 2.252302 MeV. Lower-right: the scattering state at 4.546091 MeV, this state is not much localized but can be identified as a resonance.

solutions with orbital angular momentum from 0 to 4 can be reproduced by expansions on functions with $\ell = 0$.

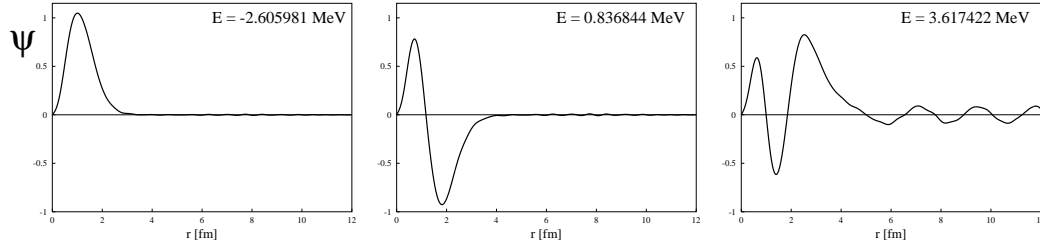


Fig. 2. Wave functions obtained for $\ell = 1$. Right: wave function of the bound state at -2.605981 MeV. Middle: the first resonance at 0.836844 MeV. Right: second resonance at 3.617422 MeV. Small unphysical oscillations can be seen on the wave functions, this phenomene is related with the behavior of the $\ell = 1$ functions near the origin, see the text for more detailed explanations.

We can also observe how the eigenfunctions behave. Some of them with $\ell = 0, 1$ and 2 are plotted on figures 1, 2 and 3. Figure 1 shows that the method is able to reproduce the deeply bound states, weakly bound states and scattering states. In the particular case of the scattering state at 2.252302 MeV, the wave function is strongly localized in the region of the potential and corresponds to a resonant state.

On figure 2 we see that the wave functions for $\ell = 1$ are less correctly reproduced. Some small unphysical oscillations appear on the tail of the functions. As it was discussed previously, this problem can be cured by enlarging the set

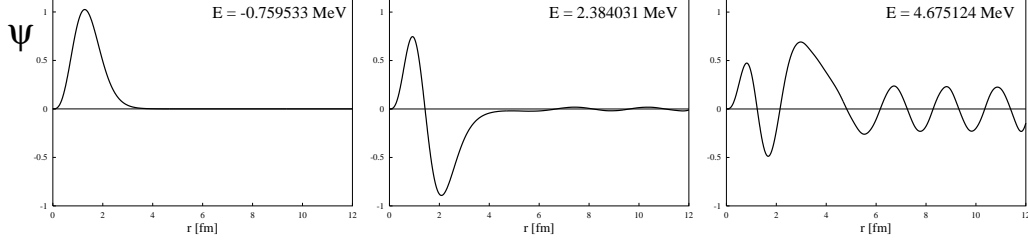


Fig. 3. Wave functions obtained for $\ell = 2$. Left: Bound state at -0.759533 MeV. Middle: Resonant scattering state at 2.384031 MeV. Right: Resonant scattering state at 4.675124 MeV. The second resonance is at higher energy so the wave function is less localized in the interior of the potential than the first one.

of functions used to expand the solutions.

We can see on figure 3 that despite the fact that the expansion of the solutions involves only functions with $\ell = 0$, the behavior of the $\ell = 0$ states at the origin ($\Psi \sim r^{\ell+1}$) is very well reproduced. One observes that the 2.384031 MeV resonance wave function is strongly localized in the region where the potential is attractive, while the 4.675124 MeV one is much less localized.

3.2 Hartree-Fock-Bogoliubov case

We choose \mathcal{U} to be a Saxon-Woods potential:

$$\mathcal{U}(r) = -\frac{\mathcal{U}_0}{1 + e^{\frac{r-R_0}{a}}} \quad (27)$$

As the pairing field is known to be mainly localized around the nuclear surface, we adopt for the particle-particle channel potential \mathcal{V} the derivative of a Saxon-Woods potential with the same radius and diffuseness as in the particle-hole channel, but with a different intensity:

$$\mathcal{V}(r) = \frac{d}{dr} \left[\frac{\mathcal{V}_0}{1 + e^{\frac{r-R_0}{a}}} \right] \quad (28)$$

The system (24) has been solved for partial waves from $\ell = 0$ to 4.

As discussed in [3], the spectrum of (24) is unbound from above and from below. The solutions for negative and positive energies are related by:

$$\begin{cases} \psi_1(-E, r) = -\psi_2(E, r) \\ \psi_2(-E, r) = \psi_1(E, r) \end{cases} \quad (29)$$

Therefore, when solving equation (24), we consider only the solutions with $E > 0$.

The numerical parameters of the particle-hole potential (28) have been taken as

$$\mathcal{U}_0 = 32 \text{ MeV}, \quad r_0 = 3.7 \text{ fm}, \quad a = 0.65 \text{ fm} \quad (30)$$

and those of the particle-particle channel potential:

$$\mathcal{V}_0 = 4 \text{ MeV}, \quad r_0 = 3.7 \text{ fm}, \quad a = 0.65 \text{ fm} \quad (31)$$

The energy scale is chosen such that $\hbar^2/2m = 20 \text{ MeV}$ in this example.

The set of functions $\{\varphi_i\}$ used to expand the solutions was generated from a box of radius 40 fm and depth 180 MeV which contains 38 bound states and 37 virtual states. The set $\{\varphi_i\}$ is built with the 38 bound states and the 2 first couples of resonances and anti-resonances, so the dimension of the matrices is 42.

ℓ	0	0	1	2
E (MeV)	-19.288	-0.856	-9.460	-0.124

Table 3

Energies of the bound states in the Saxon-Woods potential (without pairing).

In table 3 we have reported the energies and the norms of the particle-particle bound states when the pairing field and the chemical parameter are set to zero. The system has one loosely bound state 124 keV below the continuum. As mentioned in the previous paragraph, the convergence in the basis of the different partial waves is quite fast and good except for $\ell = 1$ for which it is slower. For this reason, we will present in detail the results only for $\ell=0$ and 2. As in the previous paragraph, we have checked that a satisfactory convergence for $\ell = 1$ can be obtained by enlarging the set of functions $\{\varphi_i\}$. In a future development of this method, where most general case of 3 dimensional computation will be investigated, this problem will not appear because the effective centrifugal potential is not present anymore.

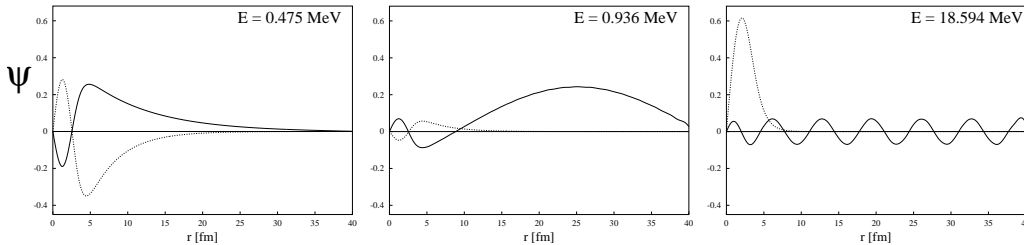


Fig. 4. Wave functions of three quasi-particle states for $\ell = 0$. The two components ψ_1 (solid line) and ψ_2 (dashed line) have the same asymptotic behaviour for the state on the left panel which corresponds to a discrete level ($E < -\lambda$), while different asymptotic behaviours are obtained for the two others which correspond to states with quasi-particle energies $E > -\lambda$.

In table 4 we have reported the energies and the norms N_2 of the lower components of the quasi-particle states for which N_2 is larger than 0.001, for $\ell = 0$ and $\ell = 2$. For higher orbital momenta, the lower component of all solutions is almost zero and does not contribute to the particle density. With the value chosen for the chemical potential ($\lambda = -0.750$ MeV), the number of particles in the system is on the average 3.163 for $\ell = 0$ and 0.417 for $\ell = 2$. We have represented in figure 4 three quasi-particle wave functions: two states close to the Fermi sea and a deep hole state, with quasi-particle energies 0.475 MeV, 0.936 MeV and 18.594 MeV, respectively. The energy of the first quasi-particle state is smaller than $|\lambda|$ and therefore this state belongs to the discrete spectrum (this is actually the only discrete state in the full spectrum). The asymptotic behaviour of the quasi-particle wave function is [3]:

$$\begin{cases} \psi_1(r) \propto \exp(-\kappa_1 r) \\ \psi_2(r) \propto \exp(-\kappa_2 r) \end{cases} \quad \text{for } r \rightarrow \infty. \quad (32)$$

The two other quasi-particle states shown in the figure are continuum states with an asymptotic behaviour given by:

$$\begin{cases} \psi_1(r) \propto \sin(k_1 r) \\ \psi_2(r) \propto \exp(-\kappa_2 r) \end{cases} \quad \text{for } r \rightarrow \infty, \quad (33)$$

with obvious definitions for k_1 , κ_1 and κ_2 .

We can see in figure 4 that the method we employ here nicely reproduces those two completely different asymptotic behaviours. Using the relation given in

$\ell = 0$				$\ell = 2$	
E (MeV)	N_2	E (MeV)	N_2	E (MeV)	N_2
0.475	0.549	4.662	0.001	1.072	0.152
0.936	0.013	15.338	0.001	1.157	0.043
1.443	0.010	18.212	0.090	1.742	0.004
2.239	0.005	18.594	0.905	2.587	0.002
3.315	0.002	21.402	0.001	3.689	0.001

Table 4

Energies E and norms N_2 of the lower components of the quasi-particle states with orbital momenta $\ell=0$ and 2. Only the states with $N_2 > 0.001$ have been reported.

equation (16) the densities of particles for $\ell=0$ and 2 can be built. These quantities are represented in figure 5 using linear and logarithmic scales.

We notice on the logarithmic plots that the behaviour of the density becomes oscillatory when it falls below 10^{-9} fm^{-3} . This is due to the truncation of the

basis expansion and also to some numerical inaccuracies. However the particle density is so small in this region that this pathology should not play any significant role in the calculation of any observable.

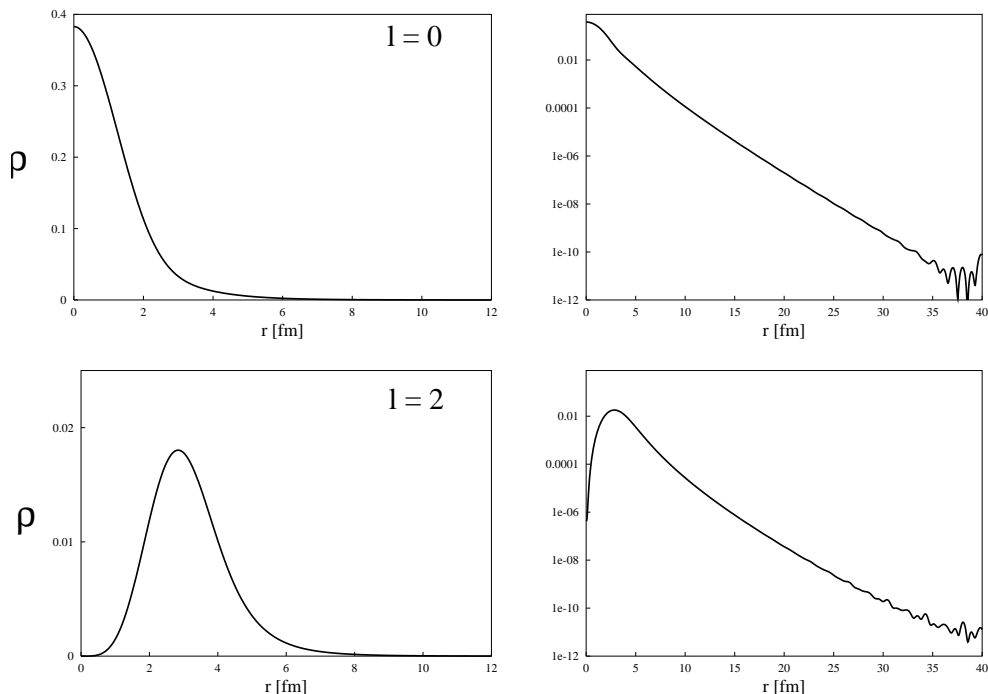


Fig. 5. Particle densities in fm^{-3} for $\ell = 0$ (top) and $\ell = 2$ (bottom) as functions of r . Figures on the right hand side are in logarithmic scale.

Eventually we diagonalize the density operator in order to construct the canonical states. The single-particle energies and occupations of $\ell = 0$ canonical states are displayed in table 5. The wave-functions of the first three ones are shown in figure 6. We notice that the expected decrease to zero at large r of these wave functions is remarkably well described within the present approach.

ϵ (MeV)	-18.570	-0.127	5.919	24.570
v^2	0.9997	0.5802	0.0012	0.0002

Table 5

Energies ϵ and occupations v^2 of the canonical states obtained for $\ell = 0$. Only the states with an occupation greater than 0.0001 have been reported.

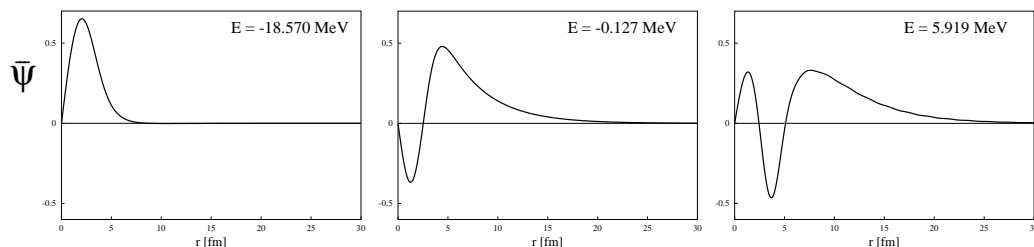


Fig. 6. Wave functions and energies of the three first canonical states for $\ell = 0$.

4 Conclusion

We have presented in this work an expansion method which can be used to express both discrete and continuum solutions of the most general HF or HFB equations, when any kind of nucleon-nucleon interaction is used. Because of the simplicity of the functions on which we expand the solutions, many steps of the resolution can be done analytically. This is the great advantage of the method. For example, the matrices needed for the resolution of the equations (12) can be evaluated analytically if the mean-field potentials are of Saxon-Woods, and derivative of Saxon-Woods or Gaussian forms.

The fact that this method avoids the problems associated with the discretization of integro-differential equations has an important consequence: it is fast and accurate. The only part of the problem that has to be done numerically is the inversion of the matrix \mathbf{R} and the diagonalisation of (12). In general, the dimension involved are rather small, at least in the case of spherical symmetry. So these steps can be done rapidly and with a good accuracy. In addition, as the quasi-particle states are expressed as finite expansions on a basis of wave-functions, the method ensures that the variational HF and HFB procedures lead to an upper bound of the total energy of the system, which can be improved at will by increasing the size of the basis.

Because of the form of the kinetic energy (15), the matrix problem that we solve is formally equivalent to solving the corresponding integro-differential equations in a box of radius r_0 with the non local boundary condition $\Psi'(r_0) = iK\Psi(r_0)$ for the solutions, where K is the operator defined by:

$$\int \varphi_m^*(r) K \varphi_n(r) dr = k_n \delta_{mn},$$

and k_n are the solutions of equation (7). In this sense, the present method is completely equivalent to working directly in the coordinate representation as done e.g. in [3] and, provided the size of the box is the same, comparable results would be obtained. The advantage of the technique we propose is that it can be applied to HFB calculations employing a finite-range nuclear interaction such as the Gogny force. Actually, once the matrix elements of the two-body force are computed, the method allows one to solve the HF and HFB equations as easily as with a basis of harmonic oscillator states, which has been done extensively with the Gogny force [2,14]. In addition, extensions of the method to non-spherical nuclei could be done in the same fashion as with harmonic oscillator bases.

Let us note that in the limit where the depth of the rectangular well goes to infinity ($V_0 \rightarrow +\infty$ in equation (4)) usual discrete Fourier expansions are recovered. In that case the formalism is greatly simplified because the tran-

scendental equation (7) becomes trivial and the overlap matrix \mathbf{R} reduces to unity.

The more general case investigated here has however the advantage of defining a reference set of functions which are adapted to the expansion of the (quasi-)particle state solutions of the HFB equations in nuclear systems. As shown in the present work, good approximation of the solutions can therefore be obtained, using comparatively small expansions.

The implementation of the present technique in the fully self-consistent HFB procedure will be the next step of this study. An important issue will be to check if nuclear properties can be accurately reproduced in realistic situations, in particular in nuclei close to drip lines, by using bases small enough to ensure extensive calculations even in heavy nuclei. If such a requirement is met, the method of solving the HFB equations we propose should open a broad range of new nuclear studies for the future.

A The decomposition of identity

In this paragraph, we consider $\hbar^2/2m = 1$ to simplify the expressions. We consider the Green function $G^{KP}(r, r'; k)$ (KP for Kapur-Peierls), corresponding to mixed boundary conditions on the domain $]0, r_0[$, solution of the (non self adjoint) problem:

$$\left\{ \begin{array}{l} \left[-\frac{d^2}{dr^2} + (V(r) - k^2) \right] G^{KP}(r, r'; k) = \delta(r - r'), \text{ if } 0 < r, r' < r_0, \\ G^{KP}(0, r'; k) = 0, \\ \frac{d}{dr} G^{KP}(r, r'; k)|_{r=r_0} = ik G^{KP}(r, r'; k)|_{r=r_0} \end{array} \right. \quad (\text{A.1})$$

If we put $p = \sqrt{k^2 + V_0}$, the solution reads:

$$\left\{ \begin{array}{l} G^{(1)}(r, r'; k) = A_1 e^{ipr} + B_1 e^{-ipr}, \text{ for } 0 \leq r \leq r', \\ G^{(2)}(r, r'; k) = A_2 e^{ipr} + B_2 e^{-ipr}, \text{ for } r' \leq r \leq r_0, \end{array} \right. \quad (\text{A.2})$$

The coefficients are given by the boundary conditions:

$$\begin{cases} G^{(1)}(0, r'; k) = 0, \\ G^{(2)}(r', r'; k) = G^{(1)}(r', r'; k), \\ (G^{(2)})'(r'_+, r'; k) = (G^{(1)})'(r'_-, r'; k) - 1, \\ (G^{(2)})'(r_0, r'; k) = ikG^{(2)}(r_0, r'; k), \end{cases} \quad (\text{A.3})$$

and we obtain:

$$G^{KP}(r, r'; k) = \begin{cases} -\frac{ik \sin p(r' - r_0) + p \cos p(r' - r_0) \sin pr}{ik \sin pr_0 - p \cos pr_0} \frac{\sin pr}{p}, & \text{if } 0 \leq r \leq r', \\ -\frac{ik \sin p(r - r_0) + p \cos p(r - r_0) \sin pr'}{ik \sin pr_0 - p \cos pr_0} \frac{\sin pr'}{p}, & \text{if } r' \leq r \leq r_0, \end{cases} \quad (\text{A.4})$$

One checks that $k \rightarrow G^{KP}(r, r'; k)$ can be meromorphically continued in the complex plane and that for $0 < r, r' < r_0$, it decays exponentially when $|k| \rightarrow \infty$ in the whole complex plane \mathbb{C} .

In order to get a completeness formula, we consider a compactly supported C^2 function f , (which is zero near the end points $r = 0$ and $r = r_0$, and we denote by g the function defined by:

$$g(r) = \left(-\frac{d^2}{dr^2} - V_0 \right) f(r). \quad (\text{A.5})$$

By multiplying (A.1) by f , (A.5) by $G^{KP}(r, r'; k)$, subtracting the two resulting equations and integrating over $(0, r_0)$, we get:

$$\int_0^{r_0} k G^{KP}(r, r'; k) f(r) dr = -\frac{1}{k} f(r') + \frac{1}{k} \int_0^{r_0} G^{KP}(r, r'; k) g(r) dr. \quad (\text{A.6})$$

By integrating on each side on a big circle $C_\Lambda = \{k \in \mathbb{C} : |k| = \Lambda\}$, we obtain:

$$\lim_{k \rightarrow \infty} \frac{1}{2i\pi} \int_{C_\Lambda} \left[\int_0^{r_0} k G^{KP}(r, r'; k) f(r) dr \right] dk = -f(r'). \quad (\text{A.7})$$

By applying the Cauchy residues theorem, we get the following formula:

$$f(r') = - \sum_n \text{Res} \left[\int_0^{r_0} k G^{KP}(r, r'; k) f(r) dr \right]_{k=k_n}, \quad (\text{A.8})$$

where the k_n are the solutions of the equation :

$$p_n \cot p_n r_0 = i k_n, \quad (\text{A.9})$$

with $p_n = \sqrt{k_n^2 + V_0}$. After computing the residue, we get the following decomposition identity:

$$f(r') = \sum_n \frac{k_n}{i + k_n r_0} \left(\int_0^{r_0} \sin p_n r f(r) dr \right) \sin p_n r'. \quad (\text{A.10})$$

In this identity, the index n labels all the complex solutions of (A.9).

One may assume for convenience that the first N roots are pure imaginary $k_n = i\kappa_n$ with $\kappa_n > 0$, and correspond to the N real eigenvalues $E_n = -\kappa_n^2$, $1 \leq n \leq N$, with $-V_0 < E_n < 0$. The other roots are located symmetrically in the negative half-plane $\Im m(k) < 0$, in such a way that if k is a root, $-\bar{k}$ is also a root of (A.9).

Numerically, the pure imaginary roots k_n can be computed by using Newton's method. For the other complex roots, one can show that [24] the behaviour of $\xi_n = k_n r_0 = x_n + i y_n$ for n large, is given by:

$$\begin{cases} x_n = c_n - \frac{1}{c_n} \log\left(\frac{2c_n}{A}\right) + \dots, \\ y_n = -\log\left(\frac{2c_n}{A}\right) - \frac{1}{2c_n^2} (\log\left(\frac{2c_n}{A}\right) - 1)^2 + \dots \end{cases} \quad (\text{A.11})$$

where $c_n = (n + \frac{1}{2})\pi$. Then $\xi_n \sim n\pi - i \log n$ gives an initial guess for the large order roots.

B Matrix elements of the potentials:

Gaussian Potential

To express the matrix elements of the Gaussian potential in compact form, we introduce the function:

$$K_{\alpha\beta}^L(\gamma) = -\frac{\exp(\beta\gamma + \frac{\gamma^2}{4\alpha})\sqrt{\pi}}{8\sqrt{\alpha}} \left[\operatorname{erf}\left(\sqrt{\alpha}\left(r - \beta - \frac{\gamma}{2\alpha}\right)\right) + \operatorname{erf}\left(\sqrt{\alpha}\left(\beta + \frac{\gamma}{2\alpha}\right)\right) \right] \quad (\text{B.1})$$

where erf denotes the error function [25]. The matrix elements of a general gaussian function:

$$f_{\alpha\beta}(r) = e^{-\alpha(r-\beta)^2}, \quad (\text{B.2})$$

can be written:

$$\begin{aligned} \int_0^L \sin(\kappa_i^* r) f_{\alpha\beta}(r) \sin(\kappa_j r) dr &= K_{\alpha\beta}^L \left(i(\kappa_i^* + \kappa_j) \right) + K_{\alpha\beta}^L \left(-i(\kappa_i^* + \kappa_j) \right) \\ &\quad - K_{\alpha\beta}^L \left(i(\kappa_i^* - \kappa_j) \right) - K_{\alpha\beta}^L \left(-i(\kappa_i^* - \kappa_j) \right). \end{aligned} \quad (\text{B.3})$$

If we choose $(\alpha = 0.25, \beta = 3.5)$ and $(\alpha = 0.2, \beta = 0)$, we can use this relation to compute the matrix element of the potential (25) very simply.

Saxon-Woods potential

In order to compute the matrix elements of the Saxon-Woods potential, we introduce the function $I_{r_0a}^L(\kappa)$ defined by:

$$I_{r_0a}^L(\kappa) = \int_0^L \frac{e^{i\kappa r}}{1 + e^{\frac{r-r_0}{a}}} dr. \quad (\text{B.4})$$

This integral can be evaluated using the hypergeometric function ${}_2F_1$ [25]:

$$\begin{aligned} I_{r_0a}^L(\kappa) &= \frac{i}{\kappa} \left[{}_2F_1 \left(1, i a \kappa; 1 + i a \kappa; -e^{-\frac{r_0}{a}} \right) \right. \\ &\quad \left. - e^{i\kappa L} {}_2F_1 \left(1, i a \kappa; 1 + i a \kappa; -e^{\frac{L-r_0}{a}} \right) \right]. \end{aligned} \quad (\text{B.5})$$

The matrix element of a Saxon-Woods potential $V(r)$ with depth V_0 , diffuseness a and radius r_0 are given by:

$$\mathbf{V}_{mn} = -V_0 \int_0^L \frac{\sin(\kappa_m^* r) \sin(\kappa_n r)}{1 + e^{\frac{r-r_0}{a}}} dr, \quad (\text{B.6})$$

and can be written explicitly using the $I_{r_0a}^L(\kappa)$ functions:

$$\mathbf{V}_{mn} = -\frac{V_0}{2} \Re \left[I_{r_0a}^L(\kappa_m^* - \kappa_n) - I_{r_0a}^L(\kappa_m^* + \kappa_n) \right]. \quad (\text{B.7})$$

If $\kappa_m^* = \kappa_n$, this expression becomes:

$$\mathbf{V}_{mn} = -\frac{V_0}{2} \left[L + a \ln \left[\frac{1 + e^{\frac{r_0}{a}}}{e^{\frac{L}{a}} + e^{\frac{r_0}{a}}} \right] - \frac{I_{r_0a}^L(2\kappa_n) + I_{r_0a}^L(-2\kappa_n)}{2} \right]. \quad (\text{B.8})$$

Derivative of Saxon-Woods potential

We have used for the particle-particle channel a potential with the shape of the derivative of a Saxon-Woods potential with depth Δ_0 , diffuseness a and radius r_0 :

$$\Delta(r) = \Delta_0 \left[\frac{d}{dr} \frac{1}{1 + e^{\frac{r-r_0}{a}}} \right]. \quad (\text{B.9})$$

The matrix elements of this potential can also be written using the function (B.5):

$$\begin{aligned} \Delta_{mn} = \Delta_0 & \left[\frac{\kappa_m^* - \kappa_n}{4i} \left[I_{r_0a}^L(\kappa_m^* - \kappa_n) - I_{r_0a}^L(\kappa_n - \kappa_m^*) \right] \right. \\ & \left. + \frac{\sin(\kappa_m^* L) \sin(\kappa_n L)}{1 + \exp(\frac{L-r_0}{a})} - \frac{\kappa_m^* + \kappa_n}{4i} \left[I_{r_0a}^L(\kappa_m^* + \kappa_n) - I_{r_0a}^L(-\kappa_m^* - \kappa_n) \right] \right] \end{aligned} \quad (\text{B.10})$$

Centrifugal term

The matrix elements associated with the centrifugal term are given by:

$$\mathbf{C}_{ij} = \frac{\hbar^2 \ell(\ell+1)}{2m} \int_0^L \frac{\sin \kappa_i^* r \sin \kappa_j r}{r^2} dr. \quad (\text{B.11})$$

This integral can be evaluated using the sine integral function [25]:

$$\mathbf{C}_{ij} = -\frac{\hbar^2 \ell(\ell+1)}{2m} \left[\frac{\sin \kappa_i^* L \sin \kappa_j L}{L} + \frac{\kappa_i^* - \kappa_j}{2} \text{Si}(\kappa_i^* - \kappa_j)L - \frac{\kappa_i^* + \kappa_j}{2} \text{Si}(\kappa_i^* + \kappa_j)L \right]. \quad (\text{B.12})$$

References

- [1] J. Dobaczewski, W. Nazarewicz, T.R. Werner, J.F. Berger, C.R. Chinn and J. Dechargé, Phys. Rev. **C 53** (1996) 2809.
- [2] J. Dechargé and D. Gogny, Phys. Rev. **C 21** (1980) 1568.
- [3] J. Dobaczewski, H. Flocard and J. Treiner, Nucl. Phys. **A 422** (1984) 103.
- [4] A. Bulgac, arXiv:nucl-th/9907088.
- [5] P. Bonche, H. Flocard, P.H. Heenen, S.J. Krieger and M.S. Weiss, Nucl. Phys. **A 443** (1985) 39.
- [6] V. E. Oberacker, A. Sait Umar, Proceedings Int. Symp. on "Perspectives in Nuclear Physics", Nassau, Bahamas, Nov. 13-17, 1998.
- [7] M.V. Stoitsov, W. Nazarewicz and S. Pittel, Phys. Rev. **C 58** (1998) 2092.
- [8] H. Kameyama, M. Kamimura, Y. Fukushima, Phys. Rev. **C 40** (1989) 974.
- [9] H. Nakada, M. Sato, Nucl. Phys. **A 699** (2002) 511.
- [10] M. Grasso, N. Sandulescu, N. Van Giai and R.J. Liotta, Phys. Rev. **C 64** (2001) 064321.
- [11] M. Grasso, N. Van Giai and N. Sandulescu, arXiv:nucl-th/0112061.
- [12] S.T. Belyaev, A.V. Smirnov, S.V. Tolokonnikov, S.A. Fayans, Yad. Fiz. **45** (1987) 1263.
- [13] K. Bennaceur, J. Dobaczewski, M. Płoszajczak, Phys. Rev. **C 60** (1999) 034308; Phys. Lett. **B 496** (2000) 154.
- [14] M. Girod and B. Grammaticos, Phys. Rev. **C 27** (1983) 2317.
- [15] B. Ducomet and C. Grojean, Rapport CEA-R-5875 (1999).
- [16] B. Ducomet and C. Grojean, Rapport CEA-R-5904 (2000).
- [17] B. Ducomet, Math. Models and Methods in the Appl. Sci. **11** (2001) 1411.
- [18] V.I. Kukulin, V.M. Krasnopol'ski, J. Horáček, *Theory of resonances*, Kluwer Academic Publishers (1989).

- [19] E. Brändas and N. Elander, Resonances, *Springer Verlag* (1989).
- [20] N. Michel, M. Płoszajczak, W. Nazarewicz, K. Bennaceur, arXiv:nucl-th/0201073.
- [21] T. Fevens and H. Jiang SIAM J. Sci. Comput. **21** (1999) 255.
- [22] P.L. Kapur and R. Peierls, Proc. Roy. Soc. **A 166** (1938) 277.
- [23] S.A. Sofianos and S.A. Rakityansky, J. Phys. **A 30** (1997) 3725.
- [24] H.M. Nussenzweig, Nucl. Phys. **11** (1959) 499.
- [25] M. Abramowitz and I. A. Stegun Handbook of mathematical functions, *Dover* (1972).